Biophysical Journal
Article

Biophysical Society

Effect of Polymer Composition and pH on Membrane Solubilization by Styrene-Maleic Acid Copolymers

Stefan Scheidelaar,[1,*] Martijn C. Koorengevel,[1] Cornelius A. van Walree,[1] Juan J. Dominguez,[1] Jonas M. Dörr,[1] and J. Antoinette Killian[1,*]

[1]Membrane Biochemistry & Biophysics, Bijvoet Center for Biomolecular Research, Department of Chemistry, Faculty of Science, Utrecht University, Utrecht, the Netherlands

ABSTRACT The styrene-maleic acid (SMA) copolymer is rapidly gaining attention as a tool in membrane research, due to its ability to directly solubilize lipid membranes into nanodisk particles without the requirement of conventional detergents. Although many variants of SMA are commercially available, so far only SMA variants with a 2:1 and 3:1 styrene-to-maleic acid ratio have been used in lipid membrane studies. It is not known how SMA composition affects the solubilization behavior of SMA. Here, we systematically investigated the effect of varying the styrene/maleic acid on the properties of SMA in solution and on its interaction with membranes. Also the effect of pH was studied, because the proton concentration in the solution will affect the charge density and thereby may modulate the properties of the polymers. Using model membranes of 1,2-dimyristoyl-*sn*-glycero-3-phosphocholine lipids at pH $>$ pH_{agg}, we found that membrane solubilization is promoted by a low charge density and by a relatively high fraction of maleic acid units in the polymer. Furthermore, it was found that a collapsed conformation of the polymer is required to ensure efficient insertion into the lipid membrane and that efficient solubilization may be improved by a more homogenous distribution of the maleic acid monomer units along the polymer chain. Altogether, the results show large differences in behavior between the SMA variants tested in the various steps of solubilization. The main conclusion is that the variant with a 2:1 styrene-to-maleic acid ratio is the most efficient membrane solubilizer in a wide pH range.

INTRODUCTION

The styrene-maleic acid (SMA) copolymer has recently gained much attention as solubilizing agent in the field of membrane protein and lipid bilayer research (for reviews, see Dörr et al. (1), Lee et al. (2), and Wheatley et al. (3)). It has been shown that this polymer is able to directly solubilize lipid membranes into nanodisk particles without the help of detergents. In this way, membrane proteins can be solubilized in their native lipid environment (4–7), which was found to help stabilize the protein (5,6,8). This has opened options to purify membrane proteins that are unstable in detergent micelles and to study native protein-lipid interactions by biochemical methods. A further advantage of these so-called native nanodisks is that they are small, with sizes in the range of 10–25 nm (4–6,9–15). This makes them suitable to be characterized by a variety of biophysical approaches including UV/Vis- and fluorescence spectroscopy (5,6,8), as well as light scattering techniques (6,14).

The SMA copolymer consists of hydrophobic styrene and hydrophilic maleic acid monomer units (Fig. 1), and variants with different monomer ratios and molecular weights are commercially available. Table 1 introduces some of these SMA variants and summarizes their physico-chemical properties. In all currently available studies using SMA for membrane solubilization and membrane protein isolation, the polymer variants used had a styrene-to-maleic acid ratio (styrene/maleic acid) of 2:1 (SMA 2:1) or 3:1 (SMA 3:1). The pH in solubilization experiments is typically in the range of 7.5–8.0, independent of the SMA variant used. The choices for using a specific SMA variant and/or pH so far have not been discussed in the literature and the effects of varying polymer composition or pH have not been investigated. Yet these parameters are likely to be important for the solubilization properties of SMA, because they determine essential factors such as hydrophobicity, ionization state, and charge density (16).

In this study, we systematically investigate the effects of polymer composition and pH on the solubilization efficiency of SMA using model membranes. 1,2-Dimyristoyl-*sn*-glycero-3-phosphocholine (di-14:0 PC) is selected as

Submitted June 21, 2016, and accepted for publication September 21, 2016.

*Correspondence: s.scheidelaar@uu.nl or j.a.killian@uu.nl

Editor: Arne Gericke.

http://dx.doi.org/10.1016/j.bpj.2016.09.025

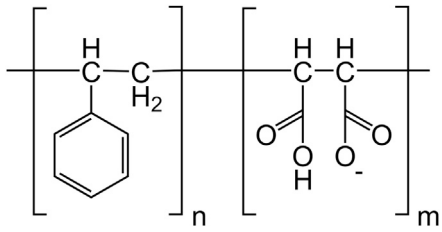

FIGURE 1 Chemical structure of the SMA polymer at 50% ionization. In this study, polymers with four different average styrene/maleic acid (n/m) = 1.4:1, 2:1, 3:1, and 4:1 have been used.

lipid because it has been used in different SMA studies where the mode of action of SMA (3,15) and the structural properties of styrene maleic acid lipid particles (14) have been characterized in molecular detail. In the systematic comparison presented here, we focus on different steps in the solubilization process of lipid membranes by SMA according to our previously proposed model (15). In brief, polymers that are initially dissolved in aqueous solution insert into the lipid membrane. The insertion of polymers then leads to membrane destabilization and subsequently to the formation of nanodisks. Along these lines, we will start by addressing some properties of SMA in solution, such as water solubility and molecular conformation of the polymers. Next, we will discuss the insertion of SMA into di-14:0 PC lipids as monitored by lipid monolayer experiments. Last, we will focus on the destabilization of membranes by SMA, which was investigated by means of a vesicle solubilization assay.

This study provides new insights into the relation between the monomer composition of SMA copolymers and their membrane-solubilizing properties, which will help to select the best SMA copolymer for the solubilization and isolation of membrane proteins from intact cells or for membrane solubilization under specific conditions such as low pH.

MATERIALS AND METHODS

Materials

Lipids were purchased from Avanti Polar Lipids (Alabaster, AL). The following two lipids were used: 1,2-dimyristoyl-*sn*-glycero-3-phosphocholine (di-14:0 PC) and 1,2-dimyristoyl-*sn*-glycero-3-phosphoglycerol (di-14:0 PG). The different styrene maleic anhydride (SMAnh) copolymer variants were a kind gift from Polyscope Polymers B.V. (Geleen, The Netherlands). All other chemicals were purchased from Sigma-Aldrich (St. Louis, MO).

TABLE 1 SMA Variants Used in this Study

Brand Name	Styrene/Maleic Acid[a]	Mol % Styrene	Mol % Maleic Acid	M_w (kDa)[b]
Xiran SZ 40005	1.4:1	57	43	5
Xiran SZ 30010	2:1	67	33	10
Xiran SZ 25010	3:1	75	25	10
Xiran SZ 20010	4:1	80	20	11

[a]Based on the acid value of the polymers as provided by the manufacturer.
[b]Values were provided by the manufacturer and are given as weight-average molecular weight, which is defined as $M_w = \frac{\sum M_i^2 \times n_i}{\sum M_i \times n_i}$.

SMA copolymer preparation

The SMA variants used throughout this study (see Table 1) were prepared in the same way as described in Scheidelaar et al. (15). Briefly, 5% (w/v) SMAnh suspensions in 1 M KOH were refluxed for ~4 h, after which the SMA was recovered by acid precipitation in 1.1 M HCl. The precipitated SMA was washed at least four times with 10 mM HCl. Finally, the SMA was dried and stored at room temperature until use. The 5% (w/v) SMA solutions were prepared by dissolving SMA powder in Milli-Q water (Millipore, Billerica, MA) while stirring and heating at 60°C. A 1 M KOH solution was slowly added until the SMA powder was completely dissolved and the solution reached pH 8.0. Finally, the obtained SMA solutions were filtered through a 0.22 μm Whatman filter (GE Healthcare Sciences, Marlborough, MA) to remove any residual particles that could possibly interfere with turbidity measurements.

Preparation of large unilamellar vesicles

Lipid stock solutions were prepared by dissolving dry lipid powder in chloroform/methanol 9:1 (v/v). Multilamellar vesicles at a concentration of 5 mM phospholipid were prepared by hydration of vacuum-dried lipid films in a 40 mM Britton-Robinson buffer (40 mM of acetic acid, boric acid, and phosphoric acid) containing 150 mM NaCl (will be referred to as standard BR-buffer) at the desired pH between 4.0 and 9.0. After hydration, at least 10 freeze-thaw cycles were performed using a dry ice/ethanol bath and a water bath set at a temperature at least 10°C above the gel-to-liquid crystalline phase transition temperature (T_m) of di-14:0 PC (T_m = 23°C). Subsequently, large unilamellar vesicles (LUVs) were prepared by extruding multilamellar vesicle dispersions at least 15 times at temperatures above T_m through a 400 nm Whatman polycarbonate filter using an Avanti Mini-Extruder (Avanti Polar Lipids). The average size of LUVs was checked by dynamic light scattering and was found to be centered at ~400 nm. Phospholipid concentrations of LUVs were determined by a phosphate assay according to Rouser et al. (17).

Determination of aqueous solubility of SMA copolymers

The solubility of the different SMA variants in water was determined in the following way. SMA solutions at a concentration of 0.1% (w/v) in a volume of 1.0 mL were prepared in a BR-buffer containing 150, 300, or 500 mM NaCl at the desired pH. The solutions were vortexed and allowed to equilibrate overnight at 20°C. Subsequently, after vortexing and 10 min equilibration, the optical density of the SMA solutions was measured at a wavelength of 350 nm using a Lambda 18 Spectrophotometer (PerkinElmer,Waltham, MA) in a 10 mm quartz cuvette holding a total volume of 900 μL. The SMA copolymer is considered to be water soluble in the pH range where an optical density of zero was observed, i.e., the value of pH_{agg} is determined as the pH value of the first examined SMA solution for which a nonzero optical density value was observed upon decreasing pH.

Acid-base titrations on SMA copolymers

Titrations on SMA copolymers were performed as follows. Milli-Q water was degassed by purging N_2 (g) through it for 30 min to remove traces of carbon dioxide. Approximately 40 mg of dried SMA was dissolved in 0.5 mL methanol and added dropwise while stirring to 50 mL degassed

Milli-Q water containing 150 mM KCl to assure a constant ionic strength during titration. A constant stream of N_2 saturated with water was gently blown above the surface of the SMA solution to prevent dissolution of carbon dioxide from the air. The temperature was kept at 25°C using a temperature-controlled water bath. The SMA solution was titrated with a 0.1 M KOH solution using a T80/50 Automatic Titration System (Schott, Mainz, Germany). A Seven Multi-pH Meter (Mettler-Toledo, Columbus, OH) was used to measure the pH after each addition of base. The pH meter was calibrated using calibration pH buffers at pH 4.0, 7.0, and 12.0 (Sigma-Aldrich). The measured pH values were corrected for possible errors caused by nonlinear electrode responses in the extreme pH regions using the Avdeef-Bucher four-parameter equation (see Supporting Materials and Methods). The corrected pH versus added volume of base curves were converted into the ionization state versus pH graphs as described in the Supporting Materials and Methods.

Nile Red fluorescence experiments

SMA solutions at a concentration of 0.1% (w/v) and a volume of 1.0 mL were prepared in a standard BR-buffer at the desired pH. A 0.25 mM Nile Red (NR) stock solution was prepared in ethanol and added to SMA solutions to a concentration of 1 μM. The critical aggregation concentration (CAC) was determined by preparing SMA solutions in a standard BR-buffer at pH 8.0 at different polymer concentrations in the range from 10^{-5} to 10 mg/mL all containing 1 μM of NR. The solutions were vortexed and allowed to equilibrate overnight at 20°C. Subsequently, NR fluorescence was measured after vortexing and 10 min equilibration on a Varian Cary Eclipse Fluorescence Spectrophotometer (Agilent Technologies, Santa Clara, CA) using a 10 mm quartz cuvette, 5 nm excitation slit, 5 nm emission slit, 1 nm resolution, 0.5 s averaging time, 120 nm/min scan speed, and a Savitzky-Golay smoothing factor of 9. The temperature was controlled with a Peltier device at 20°C. SMA solutions with NR at different pH were excited at 490 nm because at that wavelength NR molecules in a more hydrophobic environment are selectively excited (18), which is convenient for the detection of a possible collapse of the polymer chain. SMA solutions prepared at different polymer concentrations to detect a possible CAC were excited at 550 nm, as mentioned in Stuart et al. (18). The emission was recorded in the 550–700 nm region. The CAC was determined from a weighted least-square fitting using an adjusted sigmoidal function given by

$$\lambda_{\mathrm{em,max}} = B + \frac{(A-B)}{1+\left(\frac{[\mathrm{SMA}]}{\mathrm{CAC}}\right)^{n}},$$

in which A is the average $\lambda_{\mathrm{em,max}}$ before the transition, B is the average $\lambda_{\mathrm{em,max}}$ after the transition, and n is the cooperativity factor of the transition.

Lipid monolayer experiments

Surface pressure isotherms versus time were recorded for lipid monolayers of di-14:0 PC and di-14:0 PC/di-14:0 PG (1:1, molar) while adding 20 μL 5% (w/v) SMA, which represents a final concentration of 0.005% w/v. Addition of more SMA did not lead to a further increase in the surface pressure. Lipid monolayers were spread at the air-water interface by addition of a phospholipid solution (0.5 mM in 9:1 v/v chloroform/methanol) until the required initial surface pressure of 25 mN/m was reached. Solvent evaporation and equilibration of the initial surface pressure was allowed for at least 10 min before each experiment. All measurements were performed in a 6.0 × 5.5 cm compartment of a homemade Teflon trough filled with 20 mL standard BR-buffer at the desired pH at 20 ± 1°C and at constant area while stirring of the subphase. The surface pressure in time was recorded using a commercially available monolayer system (MicroTroughXS; Kibron, Helsinki, Finland). The increase in surface pressure as determined after 45 min in each experiment was reproducible within ±1 mN/m.

Vesicle solubilization experiments

The kinetics of solubilization of lipid vesicles (400 nm diameter) by the different SMA variants was monitored by turbidity measurements at 350 nm using a Lambda 18 Spectrophotometer (PerkinElmer) equipped with a Peltier element. In all experiments, a 10 mm quartz cuvette was used holding a total volume of 700 μL. The phospholipid vesicle dispersions (0.5 mM phospholipid in standard BR-buffer at the desired pH) were temperature equilibrated at 15°C for at least 10 min before addition of 15 μL of a 5% (w/v) SMA solution yielding a final SMA concentration of 0.1% (w/v). This corresponds to a SMA/phospholipid of 3:1 (w/w). SMA addition was followed by quickly mixing the contents of the cuvette using a 200 μL pipette after which the starting point was set to zero ($t = 0$). Similar time traces were obtained by stirring the solutions, but this yielded higher noise levels and was therefore avoided. Time traces of the optical density at 350 nm were reproducible for all experiments. The curves displayed in the Results are representative, and from a single experiment.

Analysis of the monomer sequence of SMA copolymers

The monomer sequences of the SMA copolymers were simulated according to the penultimate unit model with the assumption that maleic anhydride monomers do not homopolymerize (19,20). In this model, the probability P to add a styrene (= 1) or maleic anhydride (= 2) monomer unit to a growing polymer chain for which the last two monomers are either 21 or 11 is given by

$$P_{211} = \frac{\frac{F_1}{F_1-1} + \sqrt{\left(\frac{F_1}{1-F_1}\right)^2 + 4\left(\frac{2F_1-1}{1-F_1}\right)\left(\frac{r_{11}}{r_{21}}-1\right)}}{2\left(\frac{r_{11}}{r_{21}}-1\right)} \quad \text{and}$$

$$P_{112} = \frac{-F_1 + (1-F_1)\sqrt{\left(\frac{F_1}{1-F_1}\right)^2 + 4\left(\frac{2F_1-1}{1-F_1}\right)\left(\frac{r_{11}}{r_{21}}-1\right)}}{2(2F_1-1)\left(\frac{r_{11}}{r_{21}}-1\right)}.$$

Here, F_1 is the styrene fraction in the SMA copolymer of interest, and r_{11}/r_{21} is called the reactivity ratio. A value of $r_{11}/r_{21} = 0.43$ was used, as has been described by Klumperman et al. (21). Models of 50,000 polymers with 100 units each were generated and used for the analysis of styrene segments between two maleic acid units in the polymer. The results were not significantly influenced by the number of polymers and number of monomer units per polymer unless the number was reduced below 100 polymers or below 9 monomer units per polymer. The computer model was implemented and run using the free programming software JustBASIC v1.01 (Framingham, MA). The validity of our penultimate unit model was checked by constructing a styrene-centered triad fraction versus SMA composition graph. The graph was compared to the results as produced by Klumperman et al. (21) and found to be completely equal.

RESULTS

A lower styrene fraction in the polymer increases the pH range in which SMA is soluble

The preparation of nanodisks from lipid membranes is usually performed by the addition of SMA copolymers in aqueous solution to a membrane suspension. Therefore, knowledge about the aqueous solubility of SMA variants is important for determining their suitability for membrane solubilization under given experimental conditions. A particularly relevant parameter is the pH, because this determines the actual number of charges on the polymers. The pH range in which SMA is soluble is furthermore expected to vary with SMA composition, because a change in the styrene-to-maleic acid ratio alters both the overall hydrophobicity and the maximum number of charges of the polymer.

Fig. 2 *A* shows the solubility of different SMA variants as function of pH at 150 mM NaCl as monitored by turbidity measurements. In general, SMA copolymers are soluble at high pH, but become insoluble at low pH (starting at pH_{agg}) as indicated by the increase in the apparent optical density due to light scattering from aggregated polymer. The solubility range was found to be dependent on the styrene/maleic acid of the polymer, an increase in the styrene content decreasing the range in which SMA is water soluble. The SMA 1.4:1, which is the most hydrophilic polymer used, is soluble above pH 4.0, whereas the SMA 4:1, the most hydrophobic polymer used, is only completely soluble in the range from pH 7.0 to 9.0. At first sight, it might be surprising that for this polymer at pH values below 5.0, a decrease in optical density is observed. However, this does not correspond to dissolution, but instead signifies polymer precipitation.

Because negative charges on the polymer promote aqueous solubility, it is expected that an increase in ionic strength will decrease the polymer solubility due to Debye charge screening. This is indeed the case as illustrated in Fig. 2 *B* for the SMA 2:1 variant. At higher ionic strength the polymer becomes less soluble, shifting the solubility range to higher pH values. Nevertheless, at pH 7.0 or higher, the SMA 2:1 variant is soluble even at 500 mM NaCl. Reduced polymer solubility with increasing ionic strength

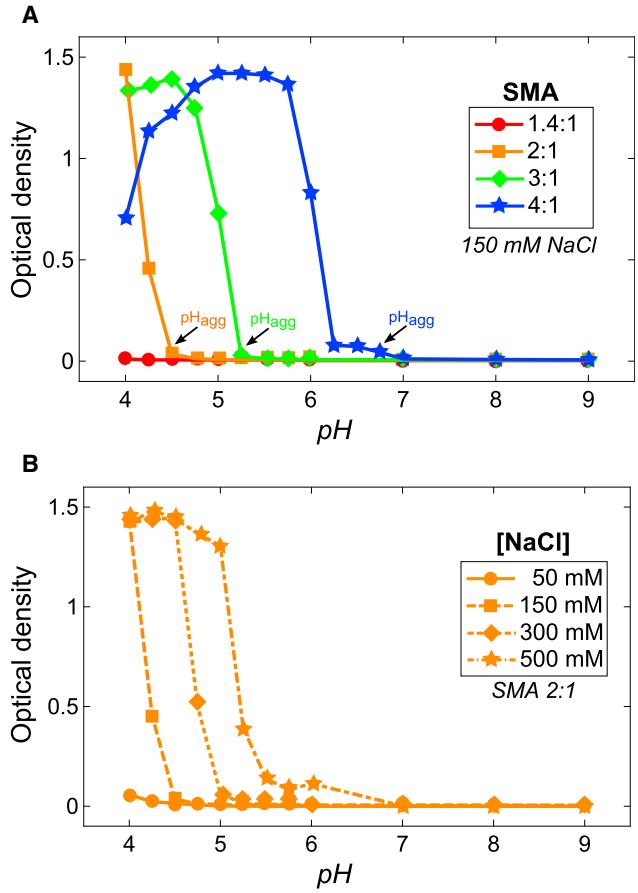

FIGURE 2 (*A*) pH dependence of optical density values of SMA solutions in standard BR buffer, which represent the solubility of the polymers. (*B*) pH-dependent optical density of solutions of the SMA 2:1 variant in BR buffer at varying ionic strength. All measurements were performed at a polymer concentration of 0.1% w/v. The optical density was measured at $\lambda = 350$ nm. Solid lines were added to guide the eye. To see this figure in color, go online.

was also found for the other SMA variants (see Fig. S1 in the Supporting Material).

In the following two sections, the physical properties of the SMA variants are studied in more detail, starting with the ionization state of the polymers.

The number of charges per unit length of polymer determines the pH range in which SMA is soluble

The charges of the carboxylic groups of the maleic acid units, and with that the ionization state of SMA, is an important factor for the aqueous solubility of the polymer as well as for the interactions between SMA and lipid membranes (15). The ionization state at a given pH is determined by the acid strength (pKa) of the acid groups in SMA. Because the pKa values of acid groups are sensitive to the nearby presence of hydrophobic groups and negative charges, it is possible that the SMA variants have different pKa values and thus different ionization states at a given pH.

A convenient way to characterize the ionization state of a polymer is to evaluate the ionization state of a monomol unit. The monomol unit is defined as the smallest unit of the polymer that represents its overall composition. This means that per monomol unit, each SMA variant will contain one maleic acid unit and a varying number of styrene units according to the styrene-to-maleic acid ratio of the polymer. In this definition, the maximal number of charges per monomol unit for each SMA variant is always two.

To determine the ionization states of the SMA variants as function of pH, acid-base titrations were performed and the obtained titration curves were converted into ionization states versus pH curves (see the Supporting Materials and Methods). For all SMA variants, a titration curve could be produced, except for the most hydrophobic SMA variant, the SMA 4:1. The poor aqueous solubility of this polymer frustrated the recording of a reliable titration curve and is therefore not presented. Fig. 3 *A* shows the protonation state (*left axis*) and corresponding ionization state (*right axis*) with the associated apparent pKa values, which are found at an ionization state of –0.5 and –1.5. The SMA 1.4:1 variant shows a steep increase in ionization between pH 4.0 and pH 5.0, after which the ionization state increases more gradually to a maximum ionization at higher than pH 11. The pKa values of the two acid groups in each monomol are well separated with a pKa_1 value at ~4.4 and a pKa_2 value at ~9.0. This large difference is caused by the short distance between the acid groups in the maleic acid units of the SMA copolymer. After ionization of the first acid group, the presence of a negative charge will cause the other acid group to be more resistant toward releasing its proton. In addition, the singly protonated state may be stabilized by an internal hydrogen bridge in the maleic acid group (22).

The 2:1 and SMA 3:1 variants show a more gradual increase in ionization state with curves that are similar in shape. The increase in styrene content decreases the acid strength of SMA as illustrated by the increase in the pKa_1 value, which is ~5.5 for the SMA 2:1 variant and ~5.9 for the SMA 3:1 variant. Despite their different monomer composition, the curves almost overlap, suggesting that the maleic acid units in both polymers experience a similar chemical environment. This similarity in chemical environment is possibly caused by a similarity in the molecular conformation of these polymers, as will be discussed later.

The pH-dependent solubility of SMA suggests a prominent role for the number of maleic acid units and their ionization state. The more hydrophobic SMA variants contain fewer maleic acids units per polymer and thus require a higher ionization state to remain water soluble, which is essential for their ability to solubilize lipid membranes. This is illustrated in Fig. 2 *B* by combining the solubility curves (Fig. 2 *A*) with the ionization state curves (Fig. 3 *B*). The obtained plot shows the optical density as a function of the average charge density along polymer chains. This linear

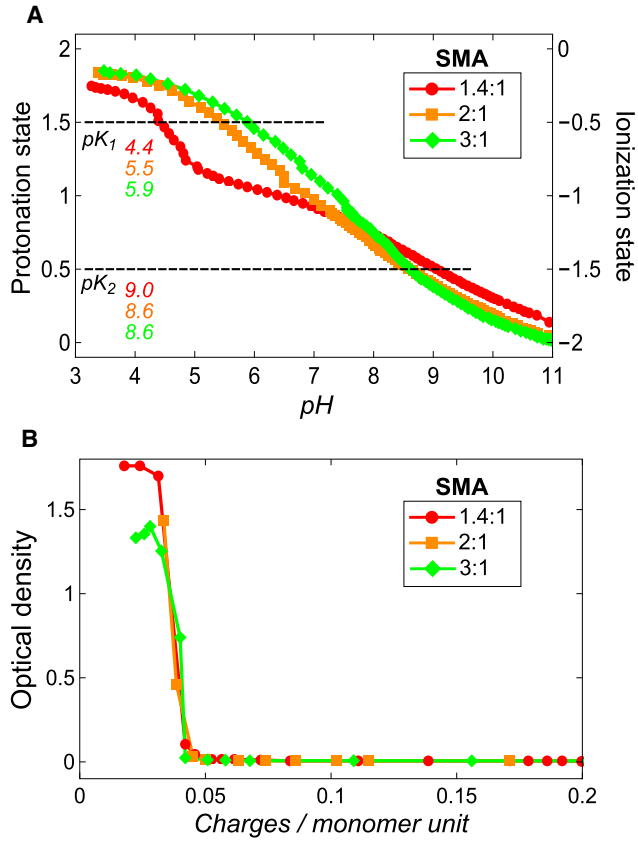

FIGURE 3 Influence of ionization state on aqueous solubility of SMA. (*A*) Protonation state (*left axis*) and corresponding ionization state (*right axis*) of the monomol of three SMA variants. The monomol is defined as the smallest unit of the polymer that represents its overall monomer composition. Titrations were performed in triplicate and gave very similar results. From the three repeated experiments the maximum error in pKa values is estimated to be ±0.2. For clarity, only a single representative ionization curve is shown for each SMA variant. (*B*) Aqueous solubility of the SMA variants as function of the linear charge density, which is given as the number of charges per monomer unit where a monomer unit represents either maleic acid or styrene. This graph was prepared by combining the results that are shown in Figs. 2 *A* and 3 *A*. Solid lines were added to guide the eye. To see this figure in color, go online.

charge density is given as the number of charges per monomer unit, where a monomer unit represents either maleic acid or styrene. For each of the three SMA variants tested, the aggregation point was found to be at ~0.045 charges per monomer unit. This means that the aqueous solubility of SMA is mainly governed by the linear charge density of the polymer, which in turn is determined both by the pH and the styrene content of the polymer.

A decrease in pH or an increase in the styrene fraction in the polymer induces a conformational change in SMA

Because water is a poor solvent for the hydrophobic styrene units in SMA, the polymer may adapt its conformation to

minimize energetically unfavorable styrene-water contacts. Indeed, in previous studies it was found that at low pH the 1:1 SMA variant collapses into a globular conformation that contains hydrophobic domains while the polymer is still water soluble (23). Such hydrophobic domains may occur within one polymer chain, but they also may be formed as a consequence of intermolecular interactions, when the polymers are present in aggregates containing multiple polymer chains termed "polymeric micelles" (24,25), as will be discussed later. Because the conformational state of the polymers is likely to be important for their interaction with lipid membranes, it was investigated how polymer conformation may be affected by the styrene/maleic acid and pH.

The conformational behavior of the SMA copolymers was studied using the lipophilic fluorophore NR. This fluorophore is solvatochromic, which means that its absorption and emission spectra are sensitive to the polarity of the environment in which it resides. In water, NR emits ~660 nm with low intensity, but when it resides in a hydrophobic solvent like t-butanol, NR shows an emission of ~620 nm with relatively high intensity (18). Thus, when SMA collapses into a conformation that contains hydrophobic domains, NR should be able to partition into those domains and show a blue shift in emission accompanied by an increase in intensity.

Fluorescence spectra of SMA solutions that contain NR at pH 8.0 are shown in Fig. 4 *A*. The excitation wavelength chosen was at 490 nm, because at this wavelength, NR molecules that are present in a hydrophobic environment are selectively excited; this makes it convenient to detect a collapsed polymer conformation (18). For the SMA 1.4:1 variant, the emission intensity under these conditions is very low with the emission maximum positioned at ~655 nm, indicating that the NR molecules reside in an aqueous environment. However, when the styrene/maleic acid of SMA increases to 2:1 and above, the maximum emission wavelength shifts to lower values and the emission intensity increases dramatically. This means that at least a fraction of the NR molecules experience a more hydrophobic environment, which may then indicate the collapsing of the polymer chain containing hydrophobic domains into which the NR molecules have partitioned. The increase in blue shift and intensity of the emission maximum with increasing styrene fraction of SMA is likely to be caused by an increase in the size and/or number of the hydrophobic domains in the polymer.

To determine how the conformational behavior of SMA is related to pH, the maximum emission wavelength is plotted versus the pH range in which the SMA variants were found to be water soluble (Fig. 4 *B*). Above a pH of 6.0, the SMA 1.4:1 variant shows maximum emission wavelengths values ~655 nm. However, from pH 6.0 to pH 4.0 the emission maximum decreases to a value of ~615 nm, consistent with a transition of NR to a more hydrophobic environment.

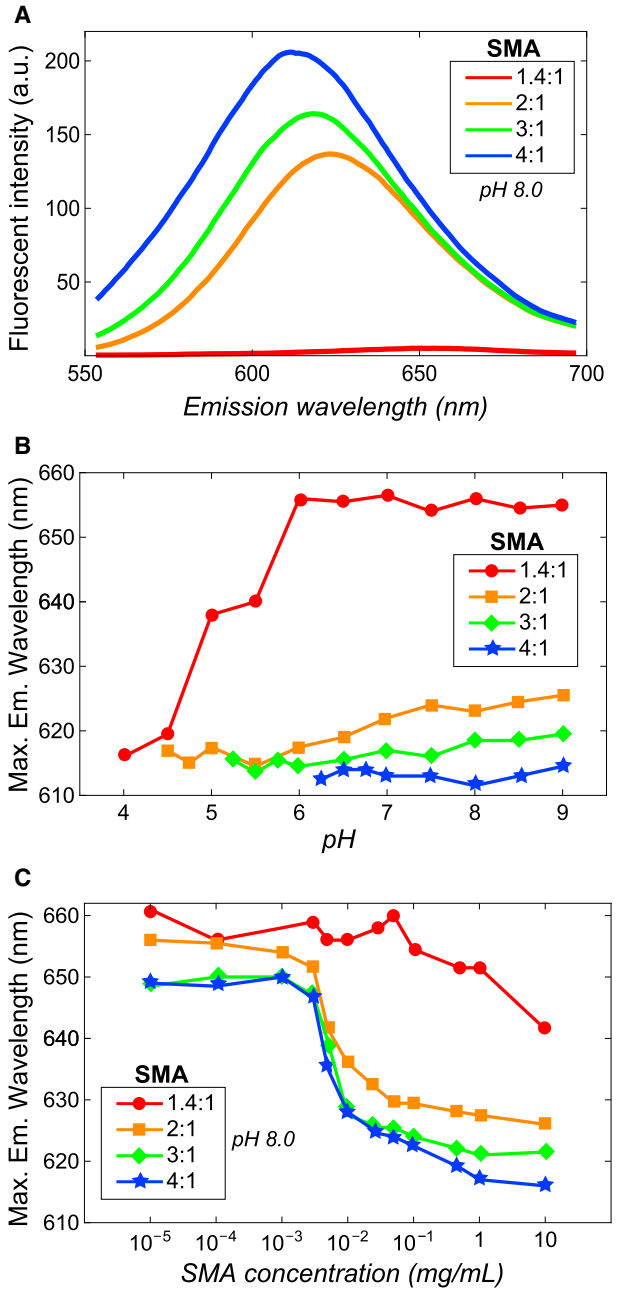

FIGURE 4 Fluorescence of NR in SMA solutions to probe polymer conformation. (*A*) Emission spectra of NR in 0.1% w/v SMA solutions at pH 8.0 excited at 490 nm. (*B*) Maximum emission wavelength as function of pH in 0.1% w/v SMA solutions ($\lambda_{ex} = 490$ nm). (*C*) Maximum emission wavelength as function of SMA concentration ($\lambda_{ex} = 550$ nm). The CAC values for the 2:1, 3:1, and SMA 4:1 variants found to be 5.8, 5.9, and 5.9 μg/mL, respectively. For SMA 1.4:1, a CAC could not be determined in this concentration range. In (*B*), only the pH range is shown where the SMA variants were found to be water soluble according to Fig. 2 *A*. The maximum emission wavelengths were estimated to have a maximum error of ~$\pm$1 nm ($n = 3$), except for the SMA 1.4:1 variant in (*C*), where the error is larger ($\pm$3 nm) due to very low emission intensities. Solid lines were added to guide the eye. To see this figure in color, go online.

Remarkably, the polymer is still well dissolved at this low pH, although it has become progressively protonated. A likely explanation for these results is a transition from an extended coil conformation of the polymer at high pH to a collapsed conformation at low pH.

The more hydrophobic SMA variants show a completely different trend than the SMA 1.4:1 variant. Despite the relatively high charge density at pH 9.0, the emission maxima are low with values between 615 and 625 nm, suggesting the presence of hydrophobic domains. An increase in styrene content of the polymer leads to a lower emission maximum because of the increase in size and/or number of the hydrophobic domains. The small decrease in emission maximum at lower pH values can simply be explained by the decrease in linear charge density of the polymer that decreases the polarity of the polymer. At low pH, close to the point where these polymers start to become insoluble in water, the emission maxima converge to the same value of ~615 nm for all SMA variants.

The presence of hydrophobic domains leads to the formation of polymeric micelles

Polymeric micelles are particles that consist of multiple polymer chains. Their formation is the result of intermolecular interactions driven by the balance in the hydrophobic effect and electrostatic repulsions (25). The existence of polymeric micelles can be detected by monitoring the maximum emission wavelength of NR as function of polymer concentration (18,26). At very low concentrations of SMA, the polymers exist as single molecules. Under these conditions, NR molecules in the hydrophobic domains have a relatively hydrophilic environment leading to emission of ~650 nm. At higher concentration, the hydrophobic domains of multiple polymers may cluster together to decrease the hydrophobic surface area that is in contact with water, thereby decreasing the polarity of the environment of NR shifting the maximum emission to ~625 nm. The concentration at which a break point in the maximum emission wavelength is observed that is characteristic for the formation of polymeric micelles is, in the case of polymers, often referred to as the "CAC" (25), which is analogous to the critical micelle concentration in the case of detergents.

Fig. 4 *C* displays the maximum emission wavelength as function of polymer concentration at pH 8.0. The SMA 1.4:1 variant shows maximum emission wavelength values between 650 and 660 nm over a large concentration range without showing a clear transition. This indicates that no polymeric micelles are formed, suggesting that this SMA variant exists as single molecules. Only at 10 mg/mL (1% w/v) does the maximum emission wavelength drop below 650 nm to ~642 nm. This may indicate the start of a CAC or it may indicate the point where the polymers start to physically influence each other due to crowding effects.

The other three SMA variants do show a clear transition in emission maximum as a function of concentration, and all three were found to have a similar CAC value of ~5.9 μg/mL. This is in accordance with the formation of polymeric micelles for these variants that already takes place at very low polymer concentration. Despite the difference in styrene content and linear charge densities of these polymer variants, the similar CAC values suggest that their polymeric micelles may be similar in molecular structure.

It is important to note here that the solubility experiments were performed at 1 mg/mL (0.1% w/v), a concentration where these SMA variants exist in the form of polymeric micelles rather than as single polymer chains. The same holds for typical lipid monolayer insertion and membrane solubilization experiments, which also were performed above the CAC of SMA and may have consequences for the interactions between SMA and lipids.

Insertion of SMA into a lipid monolayer is determined by electrostatic interactions and polymer conformation

One of the steps in the proposed model for the solubilization of lipid membranes by SMA is the insertion of the polymer into the membrane (15). The effect of SMA composition and pH on insertion can be conveniently monitored by lipid monolayer experiments.

Fig. 5 *A* shows the time traces of the insertion of the different SMA variants in a di-14:0 PC lipid monolayer at pH 8.0 and at an initial surface pressure of 25 mN/m. The SMA 1.4:1 variant is able to insert into the lipid monolayer, but increases the surface pressure only by $\approx$5 mN/m. The other SMA variants also insert but induce a remarkably large increase in surface pressure of $\approx$17 mN/m. Despite their different styrene content and linear charge density, the 2:1, 3:1, and SMA 4:1 variants all show similar insertion behavior at pH 8.0.

The effect of pH on insertion of the polymers is summarized in Fig. 5 *B* where the increase in surface pressure is shown as function of pH (see Fig. S2 for full traces). The SMA 1.4:1 variant shows a strong pH-dependent insertion behavior. At high pH the increase in surface pressure is relatively low, with a value of $\approx$5 mN/m. However, a drop in pH causes the insertion to increase drastically, as demonstrated by the large surface pressure increase of $\approx$20 mN/m at pH 5.0 and 4.0. The surface pressure increase at lower pH can be ascribed to the presence of hydrophobic domains present in the collapsed state of the polymer at low pH. These domains can insert into the lipid monolayer. In addition, the decrease in charge density at lower pH reduces electrostatic repulsions between single polymer chains at the membrane surface and in solution, allowing more polymers to insert. The latter is consistent with the notion that electrostatic interactions are an important factor for the

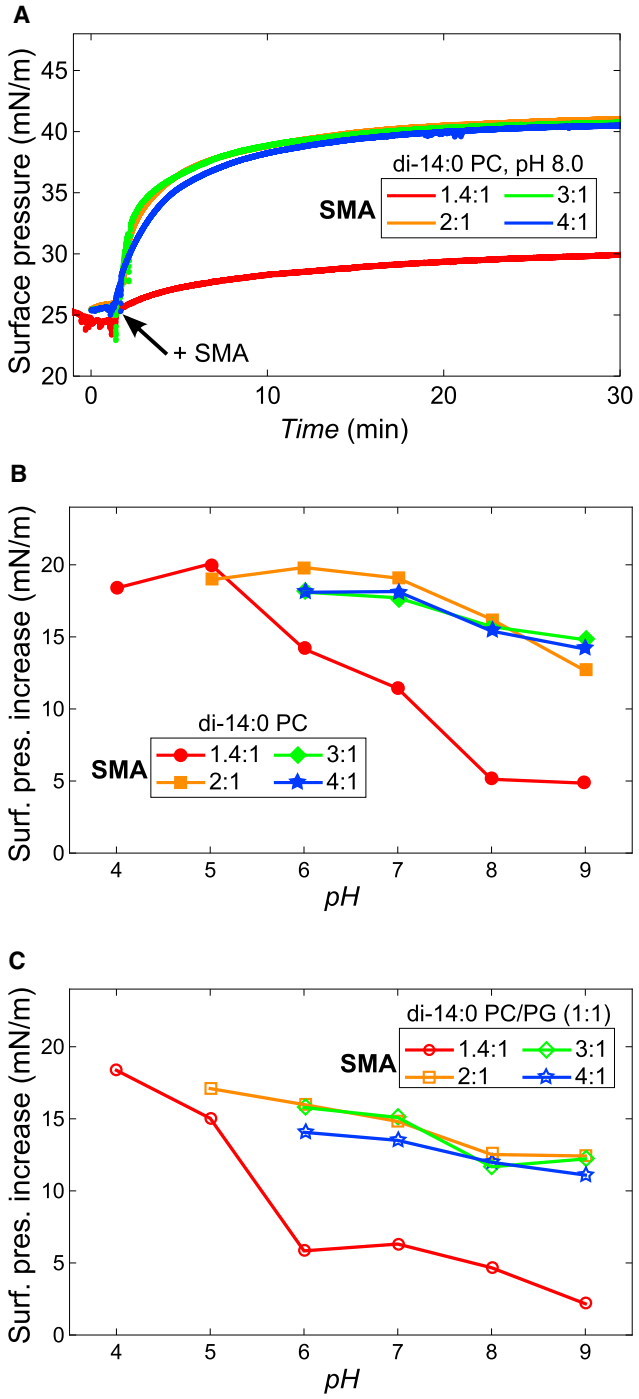

FIGURE 5 Effect of SMA composition and pH on the insertion into a lipid monolayer. (*A*) Insertion of the SMA variants into a di-14:0 PC lipid monolayer at pH 8.0. (*B*) pH-dependent insertion of the SMA variants into a di-14:0 PC monolayer. (*C*) pH-dependent insertion of the SMA variants into a di-14:0 PC/PG (1:1) monolayer. In (*B*) and (*C*), only the data points are shown where no polymer precipitation was observed during the time course of the experiment. The maximum increase in surface pressure was determined from the time point at which the signal was found to be stable, mostly at ~45 min. In all experiments the initial surface pressure was 25 mN/m, a standard BR-buffer was used, and the SMA concentration was 0.005% (w/v). Subsequent addition of more SMA did not increase the observed surface pressure any further, demonstrating that the experiments were performed under conditions of excess SMA. The maximum error in surface pressure increase for each experiment is estimated to be ± 1 mN/m as determined from repeated experiments ($n = 2$ or $n = 3$). Solid lines were added to guide the eye. To see this figure in color go online.

insertion of SMA copolymer into a lipid monolayer, as observed before for a SMA 2:1 variant (15).

The more-hydrophobic SMA variants show a large increase in surface pressure already at pH 9.0 (≈15 mN/m), which increases by an additional 2 or 3 mN/m when the pH is lowered to 6.0. Remarkable is the similar insertion behavior of the 2:1, 3:1, and SMA 4:1 variants in a wide pH range. Differences in insertion between these variants were initially expected because an increase in their styrene content will increase the hydrophobicity and will decrease the linear charge density of the polymer. By contrast, the similar pH-dependent insertion of these three polymers might suggest that despite their different monomer compositions, the overall charge density on the outside of their polymeric micelles is rather similar.

This is supported by results obtained by repeating the monolayer experiments using a lipid mixture containing 50 mol % of the negatively charged di-14:0 PG lipid (Fig. 5 *C*). In this case, the absolute values for the increase in surface pressure are lower due to increased electrostatic repulsion between SMA and PG lipids. However, the trends of surface pressure increase versus pH for the different SMA variants are again very similar.

In summary, efficient insertion of the SMA copolymer into the lipid monolayer only seems to happen under the conditions where the polymer has a collapsed state that contains hydrophobic domains. A decrease in pH allows, then, more polymer to insert due to the reduction of electrostatic repulsion between SMA copolymers. In the next section, the solubilization efficiency of di-14:0 PC vesicles is investigated to test whether the trends observed for polymer insertion also hold for the complete solubilization process.

The SMA 2:1 variant is the most efficient solubilizer of di-14:0 PC vesicles

The solubilization of di-14:0 PC vesicles by SMA was monitored by turbidimetry at 15°C, at which temperature the lipids are in the gel phase. Under these conditions, solubilization by the SMA copolymer is significantly slowed down as compared to the situation when lipids are at the gel-to-liquid-crystalline phase temperature (T_m) or in the liquid-crystalline phase (15). The slower solubilization in the gel-phase allows a convenient comparison of the effects of monomer composition and pH on the efficiency of solubilization.

Fig. 6 *A* shows the solubilization in time of the different SMA variants at pH 8.0. The SMA 1.4:1 does not solubilize the vesicles efficiently. After a quick initial drop, the optical density stabilizes and no further solubilization is observed.

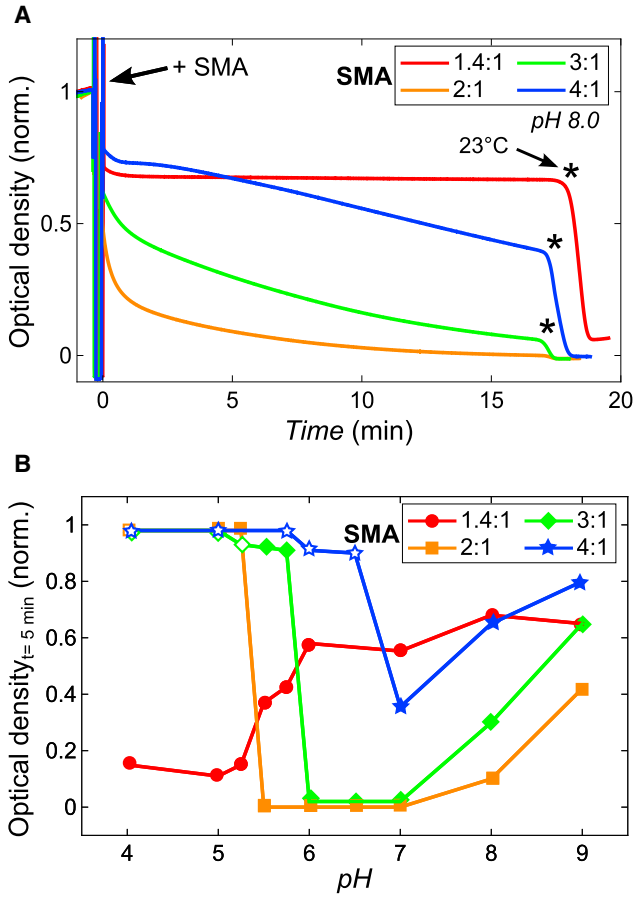

FIGURE 6 Efficiency of different SMA variants in solubilizing lipid vesicles. (*A*) Time course solubilization of di-14:0 PC vesicles in standard BR-buffer at 15°C (gel phase) by the SMA variants at pH 8.0. The asterisks denote the time where the temperature was set to 23°C, which is the T_m of di-14:0 PC. (*B*) Normalized optical density values of the di-14:0 PC vesicle suspension 5 min after SMA addition. The open symbols in (*B*) indicate that the polymer is not water soluble in the absence of lipids according to Fig. 2 *A*. Experiments where the optical density increased above the value before SMA addition have been set to a value of 1 to enhance the clarity of the figure. The relative optical density values could be reproduced with a maximum error estimated to be ± 0.05 A units ($n = 3$). All measurements were performed at a polymer concentration of 0.1% (w/v). Solid lines were added to guide the eye. To see this figure in color, go online.

When the temperature is increased to the T_m at 23°C (27) (marked by the *asterisk*), the optical density reduces quickly, showing fast and complete solubilization. This fast solubilization is attributed to the large surface defects that exist in the membrane at T_m, which makes it easy for the polymers to enter into the hydrophobic core and induce nanodisk formation (15). Solubilization at T_m can therefore be used as a control to show that any slow solubilization is due to an inability of the polymer to efficiently insert and destabilize the membrane, rather than an inability of the polymer to form nanodisks.

Fig. 6 *A* furthermore shows that the SMA 2:1 variant solubilizes the vesicles efficiently at pH 8.0, clarifying the vesicle suspension within 20 min. However, when the styrene/maleic acid of the polymer increases, the rate of solubilization decreases again. Nevertheless, both the 3:1 and SMA 4:1 variant display fast solubilization at T_m. Because the 2:1, 3:1, and SMA 4:1 variants also show similar insertion behavior (Fig. 4 *B*) the difference in solubilization between these polymers seems to be determined mainly by the solubilization step where the membrane is destabilized.

The influence of pH on membrane solubilization by the different SMA variants is shown in Fig. 6 *B* (see Fig. S3 for full traces). The SMA 1.4:1 variant solubilizes poorly at high pH, but shows a steep increase in solubilization efficiency when the pH drops below 6.0. This may be ascribed to the increased insertion of the polymer in the membrane (Fig. 5 *B*). This insertion is promoted by the presence of hydrophobic domains in the collapsed conformation of the polymer at low pH (Fig. 4 *B*), and by the decrease in charge density (Fig. 3 *A*) reducing electrostatic repulsions.

The three hydrophobic SMA variants all show a similar trend: poor solubilization at high pH; an increase in efficiency upon decreasing pH, most likely as a consequence of reduced repulsive electrostatic interactions between polymers; and no solubilization at low pH, due to insolubility of the polymers in water. However, there are two distinct differences among these SMA variants. First, the efficiency of SMA to solubilize membranes increases with an increase in the maleic acid content, most clearly visible in the pH range from 7.0 to 9.0. Second, the pH range in which the SMA variants show vesicle solubilization becomes wider with an increase in their maleic acid content, which can be ascribed to an increase in their water solubility.

The open symbols in Fig. 6 *B* denote the pH values where SMA was found to no longer be water soluble (i.e., below pH_{agg}, see Fig. 2 *A*). While the SMA 4:1 variant no longer solubilizes below its pH_{agg} of 6.75 as expected, the SMA 2:1 ($pH_{agg} = 4.50$) and SMA 3:1 ($pH_{agg} = 5.25$) variants surprisingly could not induce solubilization at pH 5.25 and pH 5.75, respectively, where these variants are still water soluble. A possible explanation for this could be that at the membrane surface, high local concentrations of polymer promote polymer-polymer interactions. Especially at the verge of water solubility, where the polymers are rather hydrophobic, these polymer-polymer interactions may compete with the ability of the polymer to solubilize or may even induce aggregation of the polymer-coated vesicles.

The styrene-to-maleic acid ratio poorly represents the monomer sequence along the polymer chain

To gain further insight into the nature of the differences in solubilization behavior between the 2:1, 3:1, and SMA 4:1 variants, the monomer sequence of SMA was analyzed. The SMA variants used in this study have styrene/maleic acid in the range from 1.4:1 to 4:1. This ratio reflects the

average fraction of the monomer units in the polymer, but does not specify anything about the monomer sequence. Yet, this might be an important factor for the mode of action of SMA; for example, a hypothetical polymer chain that has only two separate blocks, one consisting of polystyrene and one consisting of polymaleic acid, is expected to have very different solubilization properties than a polymer with perfectly alternating monomer units.

The monomer sequence of a SMA copolymer is determined by the polymerization kinetics of the styrene and maleic anhydride monomers. The polymerization process can be described by the so-called penultimate-unit model (19,20). In brief, this model implies that the chances of whether a styrene or maleic anhydride monomer is added to a growing polymer chain is determined by (1) the styrene/maleic acid of the polymer, and (2) the composition of the last two monomers on the growing chain. Another property of the polymerization of SMA copolymers is that maleic anhydride never adds to a maleic anhydride on the growing chain (19,20). This means that neighboring maleic acid units in the SMA copolymer are virtually nonexistent.

The monomer sequence of the SMA variants used here was modeled by simulating SMA copolymer formation according to the penultimate-unit model with the assumption that maleic anhydride monomers do not homopolymerize. From the simulated polymers that all had a length of 100 monomer units (see Materials and Methods for more details), the number of adjacent styrene monomer units in each styrene segment between consecutive maleic acid units was counted. If the monomer sequence would be perfectly represented by the styrene/maleic acid, for instance, the SMA 2:1 variant would then have two adjacent styrene monomer units between every two maleic acid units along the polymer chain: MA-*S*-*S*-MA-*S*-*S*-MA-*S*-*S*-MA-, etc.

Fig. 7 shows the relative abundance of styrene monomer units that are present in styrene segments of different length. The SMA 1.4:1 variant consists mainly of styrene segments of one and two styrene units (example of a possible monomer sequence in that case: MA-*S*-*S*-MA-*S*-MA-*S*-MA-*S*-*S*-MA-, etc.). However, the SMA 2:1 variant has only ~35% of all styrene monomer units in a segment of two. The 2:1 styrene/maleic acid of this polymer thus poorly represents the monomer sequence because most of the incorporated styrene units are present in longer or shorter styrene segments. This becomes progressively worse when the styrene fraction in SMA increases. The distribution of styrene segments increases and the distribution becomes much broader. Some polymers of the SMA 4:1 may even contain styrene segments that are 12 styrene-monomer-units long. Thus, analysis of the polymer sequence shows that an increase in the styrene fraction of SMA not only leads to a lower number of maleic acid units per polymer chain, but also leads to a more heterogeneous distribution of these maleic acid monomer units. The possible influence of the monomer sequence on membrane solubilization will be addressed in the Discussion.

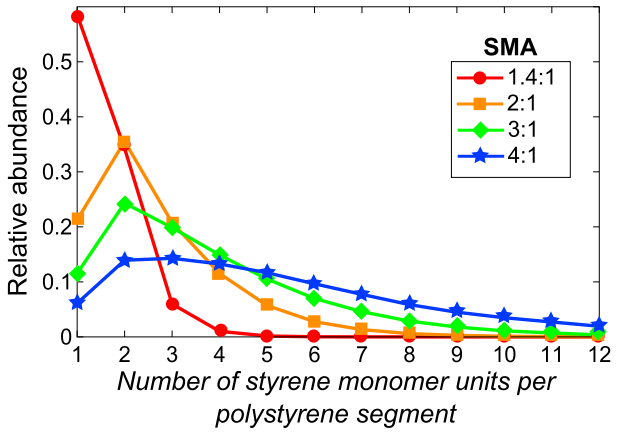

FIGURE 7 Analysis of the monomer sequence of the SMA variants. The distribution of styrene monomer units is shown as a function of the length of the polystyrene segment they are found in. Each polystyrene segment connects two consecutive maleic acid units. Polymer models were generated according to the penultimate unit model with the assumption that neighboring maleic acid units are nonexistent (see Materials and Methods and references therein for details of this model). Solid lines were added to guide the eye. To see this figure in color, go online.

DISCUSSION

Previous studies on SMA and lipid membranes all described the use of either the 2:1 or the SMA 3:1 variant at a pH in the range of ~7.5–8.0. However, it is not clear whether these were the optimal choices, because the effects of varying the styrene-to-maleic acid ratio or pH had not been investigated. In this study, we aimed at understanding how SMA composition and pH affect the molecular conformation and solubilization properties of SMA. We discuss the results of the different SMA variants tested according to Fig. 8, which is a schematic overview that summarizes the outcomes of the experiments. Finally, we suggest how the SMA copolymer might be improved in its composition to increase its solubilizing efficacy.

The SMA 1.4:1 variant

The SMA 1.4:1 variant clearly has properties very different from the other SMA variants. It is the most hydrophilic variant used and unlike the other variants, it is water soluble over the whole pH range from 4.0 to 9.0, as demonstrated by the solubility experiments. NR fluorescence experiments revealed that at a pH of ~5.5, this polymer variant undergoes a conformational change from a random coil at high pH to a collapsed conformation in which the polymer contains hydrophobic domains at low pH. A likely explanation for this pH dependence is that the decrease in ionization state and thus charge density of the polymer upon going from pH 6.0 to 4.0, as determined by acid-base titration, shifts the balance between electrostatic repulsions favoring the random coil conformation at high pH and the hydrophobic effect favoring the collapsed conformation at low pH.

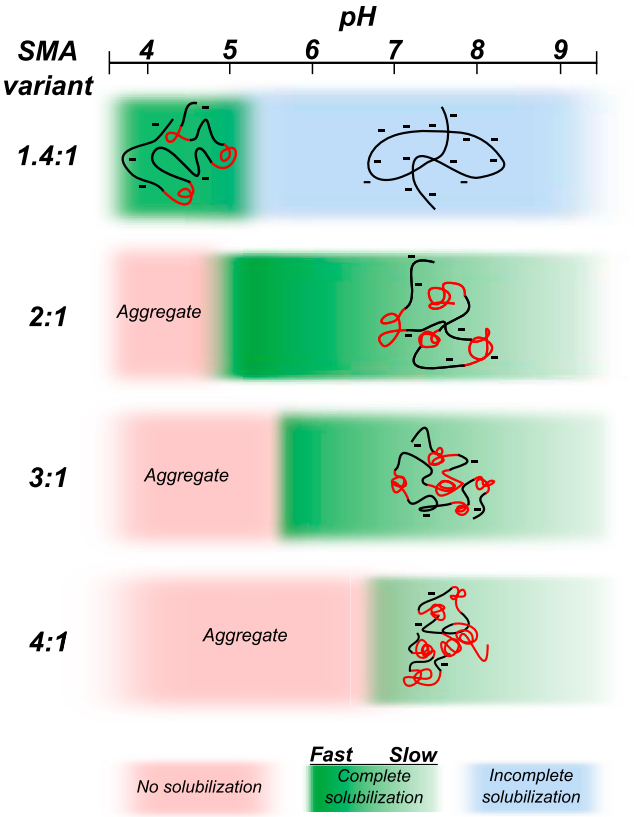

FIGURE 8 Schematic diagram that summarizes the effect of SMA composition and pH on the molecular conformation and solubilization efficiency of the SMA copolymer. The polymer conformation is shown as a cartoon in which the hydrophobic domains enriched in styrene units are shown in red, while the maleic acid-rich part of the polymer is shown in black. The efficiency of solubilization is depicted according to a color coding (see above). (*Dark green*) Complete and fast solubilization; (*blue*) solubilization is induced but remains incomplete; and (*red*) the polymer is not able to solubilize at all. To see this figure in color go online.

When the polymer has a random coil conformation, it does not insert and solubilize membranes efficiently due to its high charge state (*blue region* in Fig. 8). However, when it adopts a collapsed conformation, the polymer can solubilize membranes efficiently (*green region* in Fig. 8). Under these conditions at low pH, the hydrophobic domains insert into the membrane while the lower charge density decreases repulsive electrostatic interactions between polymers, allowing more polymer to insert into the membrane. Although this polymer may not be very suitable for solubilization of (biological) membranes or membrane proteins at neutral and high pH, it would in fact be the polymer of choice for special circumstances that require a low pH.

The 2:1, 3:1, and SMA 4:1 variants

The more hydrophobic SMA variants all have similar properties that are different from the 1.4:1 variant in two ways. First, they are not soluble over the whole pH range. Instead, they aggregate at low pH (*red region*). An increase in the styrene/maleic acid narrows the pH range in which the polymers are water soluble because the linear charge density decreases as well. Second, the polymers do not adopt a random coil conformation at high pH, but they have a collapsed conformation at every pH value tested. This observed polymer conformation is in line with a previous study that showed that SMA copolymers with a 3:1 styrene/maleic acid contain hydrophobic domains in their polymer conformation as investigated by pyrene fluorescence (24). An increase in the styrene fraction of the polymer also leads to an increase in the number and/or sizes of the hydrophobic domains. This was demonstrated by NR fluorescence experiments; the more hydrophobic SMA variants showed only a small change in maximum emission wavelength over the whole pH range, and the polymers with higher styrene fractions had lower maximum emission values, indicating an increased overall hydrophobicity of the polymers. However, we should note that we cannot rule out that the collapsed conformation of SMA copolymers, in general, can actually be described by a single hydrophobic styrene-rich core that is stabilized by a hydrophilic maleic acid-rich outside, rather than by the presence of multiple hydrophobic domains. It is also possible that the polymers possess a combination of both, with the exact structure depending on many variables, such as polymer composition, ionization state, and type of solvent (25,28).

The more hydrophobic SMA variants all show efficient insertion into the membrane as observed by lipid monolayer experiments. These similarities of the polymers indicate that the presence of hydrophobic domains enriched in styrene is necessary for efficient membrane insertion. However, the absolute fraction of styrene in the polymer does not seem to be very important for insertion. This is in contrast to the solubilization of membranes, where the styrene fraction in the polymer does play a significant role. Solubilization of di-14:0 PC vesicles in the gel phase showed that an increase in the styrene fraction in general decreases the efficiency of the polymer to solubilize a lipid membrane. Because monolayer experiments showed similar insertion behaviors for these polymers, and because fast and complete solubilization was observed at the T_m of di-14:0 PC lipids (23°C), it may be concluded that the differences in solubilization efficiency between the polymers are mainly due to differences in efficiency to destabilize the membrane.

The main difference between the SMA variants is not only the absolute number of styrene and maleic acid units in the polymer, but also the distribution of these monomers along the polymer chain. We propose that these two properties are important for destabilization of the membrane and that in particular a relatively high fraction of maleic acid in the polymer promotes efficient destabilization. The absolute amount of maleic acid in the polymer is important, because it is energetically unfavorable for its carboxylic

acid groups to come into contact with the hydrophobic core of the membrane upon polymer insertion. This will speed up the thermodynamically favorable formation of nanodisks (1,29). The distribution of the monomer units is important, because a more homogenous distribution along the polymer chain can promote uncoiling of the styrene-rich hydrophobic domains (30) into the specific conformation that is required to stabilize a nanodisk. It has been shown that when bound to the nanodisk, the SMA copolymer adopts a specific uncoiled conformation, forming a rim around the lipids in which the styrene groups intercalate between the acyl chains and the maleic acid groups pointing toward the aqueous solution (14).

Altogether, our results show that the SMA 2:1 copolymer has the most beneficial properties for efficient membrane solubilization. Its hydrophobic domains ensure efficient membrane insertion, while its relatively high maleic acid content ensures a relatively homogeneous distribution of styrene and maleic acid along the polymer, leading to efficient destabilization of the membrane. Moreover, the high maleic acid fraction guarantees water solubility at pH values above 5.0, providing the broadest pH range for solubilization of all polymers tested.

CONCLUSIONS

In this study, the effects of polymer composition and pH on membrane solubilization have been systematically investigated. This will help to select the best SMA copolymer variant for solubilization of membranes and membrane proteins under specific conditions. For example, the SMA 1.4:1 would be the best option for membrane solubilization at low pH, which may be required for stabilization of specific membrane proteins. As another example, it has been shown that increasing the salt concentration may promote membrane solubilization by reducing repulsive interactions between SMA copolymers and membranes with anionic lipids (15). However, here we show that increasing the salt concentration has a risk of inducing polymer aggregation depending on the pH of the solution. Especially when using polymers with a relatively high styrene/maleic acid like the SMA 3:1 and SMA 4:1 variant this may become a problem, because, for such polymers, aggregation in the presence of salt may occur close to physiological pH. Of all tested SMA variants, the SMA 2:1 shows the most efficient membrane solubilization in a wide pH range.

All the presented results can be explained by the differences in the styrene/maleic acid of the polymers. However, at this point we cannot exclude that the deviating behavior of the SMA 1.4:1 variant is in part due to a lower weight-average molecular weight (Table 1). The SMA variants used in this study typically have a broad distribution in molecular weight (see Dörr et al. (1) for more detail) and it is not understood yet how this affects membrane solubilization. Thus, it is possible that an optimum for membrane solubilization exists for SMA molecules of a defined molecular weight/polymer chain length. The effect of polymer length on membrane solubilization is presently being investigated in our laboratory. Depending on the outcome, it may be worthwhile to consider options for the synthesis of SMA copolymers that have both a defined monomer composition and molecular weight. These polymers then would allow systematic investigation of the optimal composition and length for membrane solubilization, which may widen the range of membrane proteins from various origins that can be isolated and characterized using the SMA solubilization approach.

SUPPORTING MATERIAL

Supporting Materials and Methods and three figures are available at http://www.biophysj.org/biophysj/supplemental/S0006-3495(16)30826-8.

AUTHOR CONTRIBUTIONS

S.S., M.C.K., and J.A.K. designed research; S.S. and M.C.K. performed research; S.S., M.C.K., C.A.W., J.D.P., J.M.D., and J.A.K. analyzed data; and S.S. and J.A.K. wrote the article.

ACKNOWLEDGMENTS

We thank Pieter Hanssen and Onno Looijmans from Polyscope Polymers B.V. (Geleen, The Netherlands) for providing the SMAnh copolymers and for useful discussions on the fabrication of SMA copolymers, and we thank Eefjan Breukink for critically reading the article and providing helpful comments. We are grateful for the contributions of Maria Teresa Piane and Ilias Theodorakopoulos as master student in our group.

Financial support of the research program of the Foundation for Fundamental Research on Matter, Netherlands Organization for Scientific Research (under NWO-ECHO grant No. 711.013.005 to J.D.P.), and the seventh framework program of the European Union (Initial Training Network "ManiFold", under grant No. 317371 to J.M.D.), are gratefully acknowledged.

REFERENCES

1. Dörr, J. M., S. Scheidelaar, …, J. A. Killian. 2016. The styrene-maleic acid copolymer: a versatile tool in membrane research. *Eur. Biophys. J.* 45:3–21.
2. Lee, S. C., S. Khalid, …, T. R. Dafforn. 2016. Encapsulated membrane proteins: a simplified system for molecular simulation. *Biochim. Biophys. Acta.* 1858:2549–2557.
3. Wheatley, M., J. Charlton, …, D. R. Poyner. 2016. GPCR-styrene maleic acid lipid particles (GPCR-SMALPs): their nature and potential. *Biochem. Soc. Trans.* 44:619–623.
4. Long, A. R., C. C. O'Brien, …, N. N. Alder. 2013. A detergent-free strategy for the reconstitution of active enzyme complexes from native biological membranes into nanoscale discs. *BMC Biotechnol.* 13:41.
5. Dörr, J. M., M. C. Koorengevel, …, J. A. Killian. 2014. Detergent-free isolation, characterization, and functional reconstitution of a tetrameric K^+ channel: the power of native nanodiscs. *Proc. Natl. Acad. Sci. USA.* 111:18607–18612.
6. Swainsbury, D. J. K., S. Scheidelaar, …, M. R. Jones. 2014. Bacterial reaction centers purified with styrene maleic acid copolymer retain

native membrane functional properties and display enhanced stability. *Angew. Chemie Int. Ed.* http://dx.doi.org/10.1002/anie.201406412.

7. Prabudiansyah, I., I. Kusters, …, A. J. Driessen. 2015. Characterization of the annular lipid shell of the Sec translocon. *Biochim. Biophys. Acta.* 1848:2050–2056.
8. Jamshad, M., J. Charlton, …, M. Wheatley. 2015. G-protein coupled receptor solubilization and purification for biophysical analysis and functional studies, in the total absence of detergent. *Biosci. Rep.* 35:35.
9. Knowles, T. J., R. Finka, …, M. Overduin. 2009. Membrane proteins solubilized intact in lipid containing nanoparticles bounded by styrene maleic acid copolymer. *J. Am. Chem. Soc.* 131:7484–7485.
10. Jamshad, M., Y.-P. Lin, …, T. R. Dafforn. 2011. Surfactant-free purification of membrane proteins with intact native membrane environment. *Biochem. Soc. Trans.* 39:813–818.
11. Orwick, M. C., P. J. Judge, …, A. Watts. 2012. Detergent-free formation and physicochemical characterization of nanosized lipid-polymer complexes: Lipodisq. *Angew. Chem. Int. Ed. Engl.* 51:4653–4657.
12. Orwick-Rydmark, M., J. E. Lovett, …, A. Watts. 2012. Detergent-free incorporation of a seven-transmembrane receptor protein into nanosized bilayer Lipodisq particles for functional and biophysical studies. *Nano Lett.* 12:4687–4692.
13. Paulin, S., M. Jamshad, …, P. W. Taylor. 2014. Surfactant-free purification of membrane protein complexes from bacteria: application to the staphylococcal penicillin-binding protein complex PBP2/PBP2a. *Nanotechnology.* 25:285101.
14. Jamshad, M., V. Grimard, …, T. R. Dafforn. 2014. Structural analysis of a nanoparticle containing a lipid bilayer used for detergent-free extraction of membrane proteins. *Nanotechnology.* http://dx.doi.org/10.1007/s12274–015–0560–6.
15. Scheidelaar, S., M. C. Koorengevel, …, J. A. Killian. 2015. Molecular model for the solubilization of membranes into nanodisks by styrene maleic acid copolymers. *Biophys. J.* 108:279–290.
16. Goddard, A. D., P. M. Dijkman, …, A. Watts. 2015. Chapter 19, Reconstitution of membrane proteins: a {GPCR} as an example. *In* Membrane Proteins—Production and Functional Characterization, Vol. 556, Methods in Enzymology. A. K. Shukla, editor. Academic Press, New York, pp. 405–424.
17. Rouser, G., S. Fleischer, and A. Yamamoto. 1970. Two-dimensional thin layer chromatographic separation of polar lipids and determination of phospholipids by phosphorus analysis of spots. *Lipids.* 5:494–496.
18. Stuart, M. C. A., J. C. van de Pas, and J. B. F. N. Engberts. 2005. The use of Nile Red to monitor the aggregation behavior in ternary surfactant-water-organic solvent systems. *J. Phys. Org. Chem.* 18:929–934.
19. Klumperman, B., and K. F. O'Driscoll. 1993. Interpreting the copolymerization of styrene with maleic anhydride and with methyl methacrylate in terms of the bootstrap model. *Polymer (Guildf.).* 34:1032–1037.
20. Klumperman, B. 2010. Mechanistic considerations on styrene-maleic anhydride copolymerization reactions. *Polym. Chem.* 1:558–562.
21. Klumperman, B. 1994. Free radical copolymerization of styrene and maleic anhydride. Kinetic studies at low and intermediate conversion. Ph.D. thesis, DSM Research & Technical University Eindhoven, Eindhoven, The Netherlands.
22. Haines, T. H. 1983. Anionic lipid headgroups as a proton-conducting pathway along the surface of membranes: a hypothesis. *Proc. Natl. Acad. Sci. USA.* 80:160–164.
23. Tonge, S. R., and B. J. Tighe. 2001. Responsive hydrophobically associating polymers: a review of structure and properties. *Adv. Drug Deliv. Rev.* 53:109–122.
24. Claracq, J., S. F. C. R. Santos, …, J.-M. Corpart. 2002. Rigid interior of styrene-maleic anhydride copolymer aggregates probed by fluorescence spectroscopy. *Langmuir.* 18:3829–3835.
25. Olea, A. F. 2012. Hydrophobic Polyelectrolytes. John Wiley, New York, pp. 211–233.
26. Tang, R., W. Ji, and C. Wang. 2011. pH-Responsive micelles based on amphiphilic block copolymers bearing ortho ester pendants as potential drug carriers. *Macromol. Chem. Phys.* 212:1185–1192.
27. Silvius, D. J. R. 1982. Thermotropic phase transitions of pure lipids in model membranes and their modifications by membrane proteins. *In* Lipid-Protein Interactions. John Wiley, New York.
28. Dobrynin, A. V., and M. Rubinstein. 1999. Hydrophobic polyelectrolytes. *Macromolecules.* 32:915–922.
29. Vargas, C., R. C. Arenas, …, S. Keller. 2015. Nanoparticle self-assembly in mixtures of phospholipids with styrene/maleic acid copolymers or fluorinated surfactants. *Nanoscale.* 7:20685–20696.
30. Murnen, H. K., A. R. Khokhlov, …, R. N. Zuckermann. 2012. Impact of hydrophobic sequence patterning on the coil-to-globule transition of protein-like polymers. *Macromolecules.* 45:5229–5236.

Biophysical Journal, Volume *111*

Supplemental Information

Effect of Polymer Composition and pH on Membrane Solubilization by Styrene-Maleic Acid Copolymers

Stefan Scheidelaar, Martijn C. Koorengevel, Cornelius A. van Walree, Juan J. Dominguez, Jonas M. Dörr, and J. Antoinette Killian

Supporting Material

Effect of polymer composition and pH on the solubilization of lipid membranes by styrene-maleic acid copolymers

S. Scheidelaar, M.C. Koorengevel, C.A. van Walree, J.J. Dominguez, J.M. Dörr, and J. A. Killian

Supporting Materials & Methods

Acid–base titrations on SMA copolymers

The measured pH values were corrected for possible errors caused by non-linear electrode responses in the extreme pH regions using the Avdeef-Bucher four-parameter equation (**Eq. S1**) (1). In here, pH is the measured pH, α and k are constants, p_cH is the corrected pH, j_H and j_{OH} the parameters that account for the non-linear electrode responses in the extreme pH regions, K_w the water dissociation constant, and $[H^+]$ the corrected proton concentration. The parameters α, k, j_H, and j_{OH} were determined from weighted least squares fitting of alkalimetric titrations of known concentrations of HCl (blank titration) (1). Once the values of these parameters are known, Eq. S1 can be solved for every data point in the titration curve.

(**Eq. S1**) $pH = \alpha + k\ p_cH + j_H\ [H^+] + j_{OH}\ \frac{K_w}{[H^+]}$

Curves of the corrected pH versus the volume of added base were converted into curves of protonation state/ionization state versus pH according to **Eq. S2** in which n_H is the protonation state, $[OH^-] = 10^{(p_cH - pK_w)}$ the hydroxide concentration, $[K^+] = \frac{[KOH]}{V_{initial}+V_{added}}$ the potassium concentration, $[H^+] = 10^{-p_cH}$ the proton concentration and [SMA] the monomol concentration of the SMA variant used in the titration.

(**Eq. S2**) $n_H = 2 + \frac{[OH^-]-[K^+]-[H^+]}{[\mathrm{SMA}]}$

Figure S1

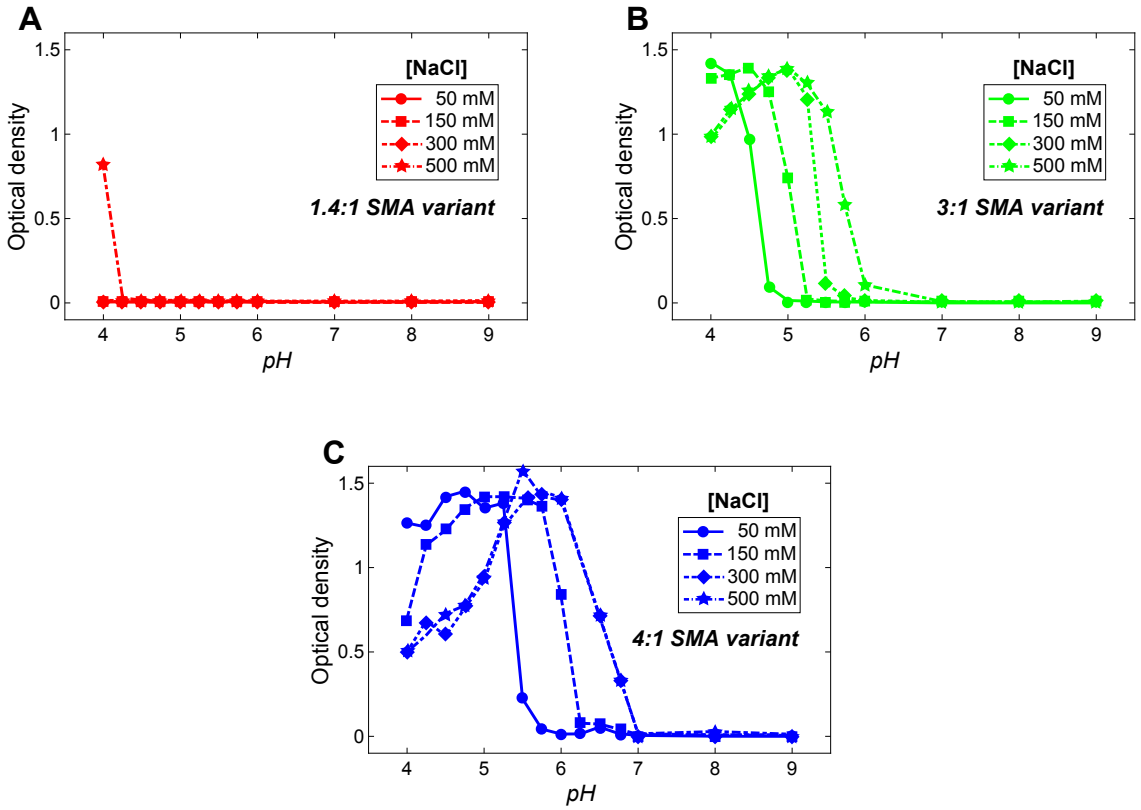

Figure 1: pH dependent solubility of different SMA variants in a 40 mM Britton-Robinson buffer at varying ionic strengths. All measurements have been performed at a polymer concentration of 0.1% (w/v). The optical density was measured at λ=350 nm. Lines have been added to guide the eye.

Figure S2

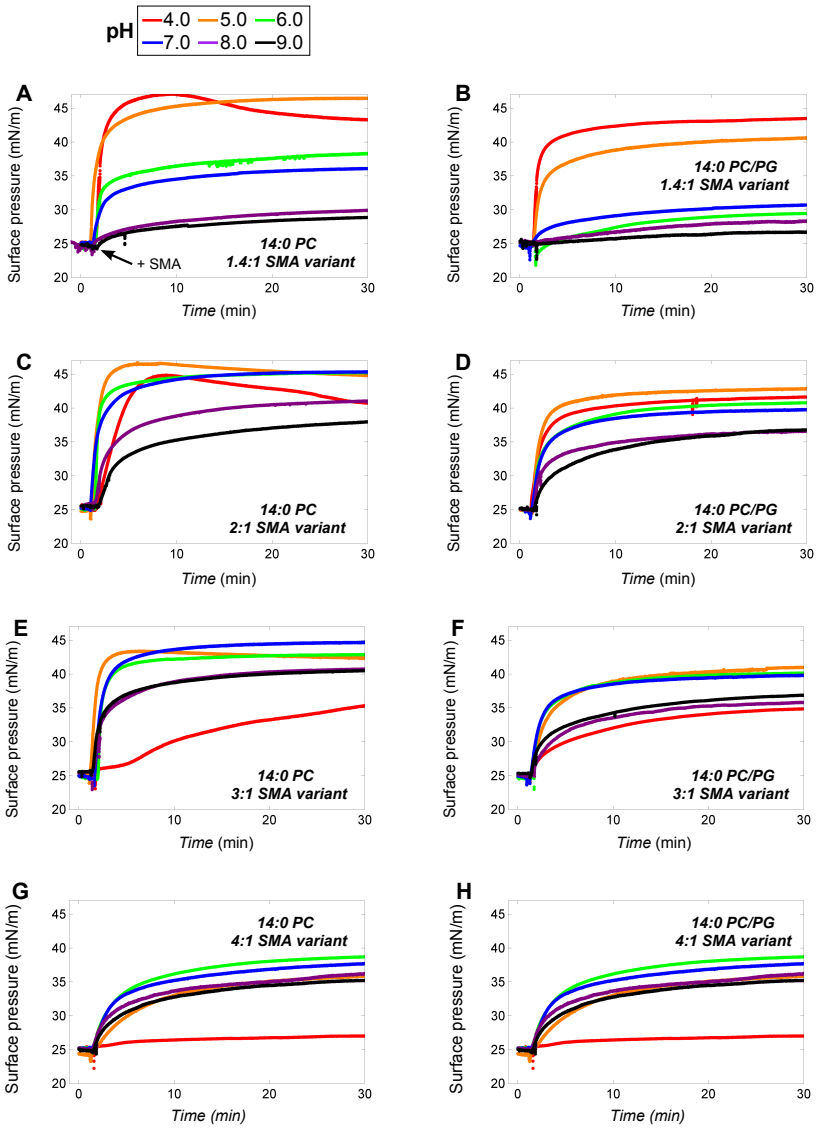

Figure 2: Insertion of the SMA variants in a di-14:0 PC and di-14:0 PC/PG (1:1 mol) lipid monolayer at different pH values. In all experiments the initial surface pressure was 25 mN/m, NaCl concentration is 150 mM and SMA concentration is 0.005% (w/v). Subsequent addition of more SMA did not increase the observed surface pressure any further, demonstrating that the experiments were performed under conditions of excess SMA.

Figure S3

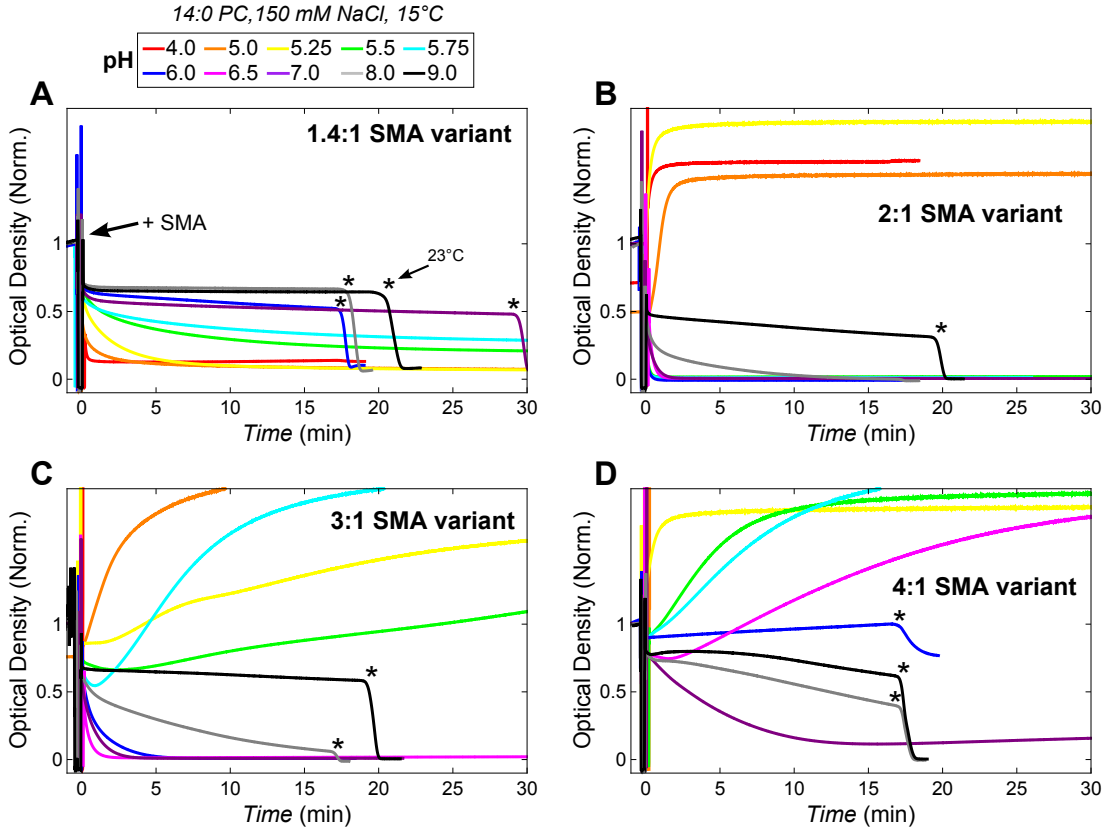

Figure 3: Time course solubilization of di-14:0 PC vesicles at 15 °C (gel phase) by each SMA variant at different pH values. The asterisks denote the time where the temperature was set to 23 °C, which is the T_m of 14:0 PC (2). For the 2:1, 3:1, and SMA 4:1 variants at lower pH, the relative optical density rises above 1. This means that the optical density increases after SMA addition, which is likely to be caused by polymer aggregation or clustering of vesicles due to the polymer. All measurements have been performed at a polymer concentration of 0.1% (w/v).

Supporting References

[1] Avdeef, A., 1983. Weighting scheme for regression analysis using pH data from acid-base titrations. *Analytica Chimica Acta* 148:237 – 244. http://www.sciencedirect.com/science/article/pii/S0003267000851685.

[2] Silvius, D. J. R., 1982. Thermotropic phase transitions of pure lipids in model membranes and their modifications by membrane proteins, volume Lipid-Protein Interactions. John Wiley & Sons, Inc. New York.